frontiers | Frontiers in Environmental Science

TYPE Original Research
PUBLISHED 07 March 2024
DOI 10.3389/fenvs.2024.1353267

OPEN ACCESS

EDITED BY
Hongzhi Ma,
University of Science and Technology Beijing, China

REVIEWED BY
Ahmed S. El-Shafie,
Qatar University, Qatar
Titus Egbosiuba,
Chukwuemeka Odumegwu Ojukwu University, Nigeria

*CORRESPONDENCE
Liaqat Ali,
liaqatbiotech@gmail.com
Sadia Aziz,
sadiaawanqau@gmail.com

RECEIVED 10 December 2023
ACCEPTED 16 February 2024
PUBLISHED 07 March 2024

CITATION
Aziz S, Anbreen S, Iftikhar I, Fatima T, Iftikhar A and Ali L (2024), Green technology: synthesis of iron-modified biochar derived from pine cones to remove azithromycin and ciprofloxacin from water.
Front. Environ. Sci. 12:1353267.
doi: 10.3389/fenvs.2024.1353267

Green technology: synthesis of iron-modified biochar derived from pine cones to remove azithromycin and ciprofloxacin from water

Sadia Aziz[1]*, Sundus Anbreen[2], Iqra Iftikhar[1], Tabassum Fatima[1], Aqsa Iftikhar[1] and Liaqat Ali[3]*

[1]Department of Biological Sciences, International Islamic University Islamabad, Islamabad, Pakistan, [2]Department of Biotechnology, Quaid I Azam University Islamabad, Islamabad, Pakistan, [3]Department of Biological Sciences, National University of Medical Sciences, Rawalpindi, Pakistan

The rise of antibiotic pollutants in water threatens ecosystems and human health. Iron-modified biochar (BC) exhibits adsorption properties and offers a promising approach for effective environmental remediation. The current study explored the potential of iron-loaded biochar synthesized from pine cones for antibiotic removal from water. In this study, pine cones, a sustainable and renewable source, were used to produce iron-modified biochar and employed to remove azithromycin, ciprofloxacin, and their mixture from aqueous solutions. Biochar was synthesized through pyrolysis and modified by the addition of iron salts. The analysis of iron-modified biochar by Fourier-transform infrared spectroscopy (FT-IR), X-ray diffraction (XRD), and scanning electron microscopy (SEM) suggested a crystalline structure rich in minerals and functional groups (O–H, C=O, and C≡C) and loaded with iron, having plate-like roughness and distorted morphology along with sharp edges and corners. Antibiotic removal was evaluated by changing physical parameters, including biochar dose, pH, and temperature. The maximum removal percentages of azithromycin, ciprofloxacin, and their mixture were obtained as 87.8%, 91.3%, and 84%, respectively, at low pH, a low Fe-modified biochar dose, and higher temperature. Application of kinetic models suggested that the adsorption of antibiotics on iron-modified biochar is more inclined toward pseudo-second-order (R^2 > 0.98) kinetics, indicating a chemisorption nature of the adsorption process. The findings highlight the potential of iron-modified biochar for removing antibiotics from aqueous solutions.

KEYWORDS

pine cones, Fe-modified biochar, azithromycin, ciprofloxacin, pyrolysis, adsorption, antibiotic removal

1 Introduction

Broad-spectrum antibiotics play a crucial role in combating diverse bacterial infections in both human and veterinary medicine (Ding and He, 2010). Although they have saved lives globally, their overuse and misuse contribute to antibiotic resistance, a serious threat to public health (Martõ et al., 2001; Kümmerer, 2003, 2009). The release of pharmaceutical residues into the environment via treated or untreated wastewater exacerbates this issue

TABLE 1 Removal efficiency of various adsorbents for azithromycin and ciprofloxacin.

Antibiotic	Adsorbent	Removal efficiency	Reference
Ciprofloxacin	Corn cob	56.3%	Peñafiel et al. (2019)
	Rice husk	59.7%	Peñafiel et al. (2019)
	Wheat bran	75%	Khokhar et al. (2019)
	Acid activated carbon	250 mg/g	Chandrasekaran et al. (2020)
	MgO nanostructures	528 mg g^{-1}	Sivaselvam et al. (2020)
	Porous graphene hydrogel	75%	Ma et al. (2015)
	Magnetic metal–organic framework	72.15%	Yu et al. (2023)
	Granular ferric hydroxide	42.31%	Asadi-Ghalhari et al. (2022)
Azithromycin	*Azolla filiculoides*-based activated porous carbon	87%	Balarak et al. (2021)
	Graphene oxide	98.8%	Upoma et al. (2022)
	Biochar with montmorillonite	44.73 mg g^{-1}	Arif et al. (2023)
	Forest soils	between 13.25% and 37.27%	Cela-Dablanca et al. (2022)
	Saponin-modified nanodiatomite	91.7 mg/g	Davoodi et al. (2019)

(Osińska et al., 2020). The World Health Organization recognizes antibiotic resistance as a major global health challenge (Dorgali et al., 2020), and the accumulation of antibiotics in the environment may lead to the development of antibiotic-resistant genes in microorganisms (Manaia, 2017).

Azithromycin and ciprofloxacin, both common antibiotics, are found as contaminants in surface water, wastewater, and soil (Mirzaei et al., 2018). Azithromycin, a macrolide, is the third most widely consumed group of antibiotics used for respiratory diseases and sexually transmitted infections, while ciprofloxacin, a fluoroquinolone, is prescribed for chest and urinary tract infections. Due to their continuous release into the environment, they are considered pseudo-persistent pollutants that pose risks to non-target organisms and impact aquatic ecosystems (Kovalakova et al., 2020).

Several conventional methods have been developed to remove antibiotics from wastewater (Sanni et al., 2023); however, these methods have limitations, such as high energy consumption, low efficiency, and the production of toxic byproducts (Phoon et al., 2020). Among various methods, adsorption for the removal of antibiotics has become an attractive method because it is cost-effective, efficient, and has low or no risk of producing toxic byproducts. Table 1 summarizes the removal of azithromycin and ciprofloxacin using various adsorbents. In recent years, the interest in utilizing biochar to eliminate pollutants has been growing. Biochar, a carbon-rich porous material derived from biomass through pyrolysis, has an eco-friendly, cost-effective nature owing to its extensive surface area, porosity, and pore volume (Hafeez et al., 2022). Porous structure, surface negative charge, and carboxyl and hydroxyl functional groups play a crucial role in binding and attracting positively charged antibiotics through hydrogen bonding and electrostatic interactions (Gasim et al., 2022). However, the efficacy of biochar as an adsorbent relies on various factors, including pH and temperature (Aoulad et al., 2023).

Different methods, such as the addition of acid and metal impregnation, have been utilized to improve biochar adsorption capabilities by enhancing surface functional groups (Chen et al., 2021). Chemical activation significantly enhances the porosity of biochar and influences its surface chemical properties, including surface functional groups, hydrophobicity, and polarity (Tan et al., 2017). Loading biochar with iron represents an advanced approach in removal studies, addressing numerous limitations encountered when using unmodified biochar. Transition metals (Fe, Co, Ni, etc.) or their oxides have recently been introduced into biochar matrices to enhance biochar adsorption capability (Han et al., 2016; Zeng et al., 2021). In addition, the magnetic separation technique can be applied to remove iron-modified biochar from aqueous solutions (Lu et al., 2020). The iron modification of biochar enhances the contact between biochar and antibiotics, facilitating their effective adsorption onto the surface of modified biochar (Li et al., 2020).

The synthesis methodology and the type of feedstock material used play pivotal roles in determining the properties and characteristics of biochar (Bhandari et al., 2023). Most of the biochar in literature is obtained from organic waste-based raw materials. Pine cones are the reproductive structures of pine trees, often considered waste materials in forestry (Sahin and Yalcin, 2017), and are abundant in many regions of the world, including the northern areas of Pakistan (Hussain et al., 2019). Pine cones contain a high proportion of carbon, which makes them a potentially valuable feedstock for Fe-modified biochar production (Zhao et al., 2020) and an effective, inexpensive, and environmentally sustainable adsorbent for environmental treatment.

Despite the significant advancements in biochar research, data on its production from pine cones and iron modification and its efficiency in azithromycin and ciprofloxacin removal from water are currently lacking. The current study focused on the physiochemical characterization of Fe-modified biochar sourced from pine cones, examining its efficacy in adsorbing and eliminating antibiotics from aqueous solutions under diverse conditions and parameters. Additionally, it provides a

comprehensive analysis of how various factors influence the removal rates of antibiotics by Fe-modified biochar, employing distinct kinetic models to outline these impacts.

2 Materials and methods

2.1 Materials

In this study, pine cones were used as a substrate to prepare biochar. Pine cones were collected from International Islamic University in Pakistan. Antibiotics selected for the removal study were azithromycin (Novartis) and ciprofloxacin (Sami), purchased from a local drug store in Islamabad. The chemicals used in the study were purchased from Sigma-Aldrich. Filter paper, syringe filters, beakers, flasks, a muffle furnace (FNC-BX 1200), a UV-visible spectrophotometer (Agilent 8453), a weighing balance (WANT, WTB 2002K), a pH meter (PHS-3C), and a shaker (DRAWELL DW-SI-100B) were the apparatus and instruments used in the study.

2.2 Preparation of biochar

Biochar was prepared from pine cones by pyrolysis (Sarkar et al., 2019). Pine cones were collected, washed, and dried in the open air for 48 h. After that, the cones were crushed into small pieces, packed into ceramic crucibles, and covered to limit their exposure to oxygen. These crucibles were then placed into a muffle furnace (5 kW power output, 280 V) and subjected to pyrolysis at 600°C for 2 h (Sarkar et al., 2019). The produced biochar was ground and sieved to less than 0.25 mm.

2.3 Iron modification of biochar

Biochar (25 g ± 0.1 g) was added to 250 mL of distilled water. Ferric chloride salt (9 g ± 0.3 g, solid) was added to 650 mL of distilled water, and 10 g ± 0.21 g of ferrous sulfate was added to 75 mL of distilled water. Both solutions ($FeCl_3$ + $FeSO_4$) were added in one flask and stirred at 65°C on the hotplate. The suspension solutions were diluted to 250 mL with water in which 25 g ± 0.1 g biochar was added and stirred for 30 min. Then, 10 M NaOH was added until the pH was raised from 10 to 11. After mixing for 1 h, the mixture was kept for 24 h at room temperature and then washed with distilled water until a neutral pH was reached. After that, the Fe-modified biochar (FMBC) was filtered on filter paper, dried in a desiccator at 37°C, and collected in a polythene bag (Nakahira et al., 2006).

2.4 Biochar and Fe-modified biochar characterization

The following formula was applied to calculate the yield of biochar and Fe-modified biochar Eq. (1) (Egbosiuba et al., 2020; Egbosiuba, 2022):

$$\text{Yield\%} = \frac{\text{mass of pine cones before pyrolysis}}{\text{mass of pine cones after pyrolysis}} \times 100. \quad (1)$$

The yield of Fe-modified biochar was determined by the following formula Eq. (2):

$$\text{Yield\%} = \frac{\text{Mass of Fe} - \text{modified biochar}}{\text{mass of biochar}} \times 100. \quad (2)$$

The Biochar and Fe-modified biochar were characterized. FT-IR spectra (FT-IR, PerkinElmer 2012) of both biochar and Fe-modified biochar samples were obtained in the wavelength range of 4,000–550 cm^{-1}. X-ray powder diffraction (XRD, PANalytical 2006 Wax.) was performed by monochromatic X-ray radiations of wavelength 1.542 Å, scanning in the range of 10°–60° (2θ) and scanning at a speed of 2° per min for both samples. The surface morphology and macropore shape of biochar and Fe-modified biochar were studied using a JSM 5910 lv thermionic scanning electron microscope (JEOL SEM, Japan) (Silva et al., 2020).

2.5 Adsorption studies

For adsorption purposes, solutions of antibiotics and their mixture were prepared, each having 2 mg ± 0.01 mg of antibiotic in 100 mL of distilled water, making a concentration of 20 mg/L, and stirred for 5 min. No additional step was taken as both antibiotics have solubility in water at this concentration and had been reported in wastewater in previous studies (Mirzaie et al., 2020). In another study, a mixture of azithromycin was prepared with a 25 mg/L concentration at neutral pH (Arif et al., 2023). Fe-modified biochar was added to these flasks and placed in a shaking incubator with a shaking speed of 150 rpm. A 4 mL aliquot of the mixture was drawn from each flask at 0 min, 30 min, 60 min, 90 min, 120 min, 150 min, and 180 min. The aliquot was filtered through a 0.22-μm syringe filter and subjected to a UV-visible spectrophotometer to measure the adsorption of antibiotics by Fe-modified biochar. The adsorption of azithromycin was measured at 205 nm, and the adsorption of ciprofloxacin was measured at 278 nm, while the adsorption was taken at both wavelengths for the mixture. The final mean was calculated for the removal of both antibiotics in the mixture.

2.5.1 Effect of different parameters on antibiotic removal

Different variables were used to analyze the adsorption capacity of Fe-modified biochar for antibiotics. As three variables were studied at a time, they were taken in binary mode, each having two categories: acidic/basic pH, low temperature/high temperature, and low dose/high dose of biochar.

2.5.1.1 Effect of pH on antibiotic removal

Solutions of NaOH and H_2SO_4 at concentrations of 1, 0.1, and 0.01 mol/L were prepared to adjust solution pH to 6 and 9. Ciprofloxacin, azithromycin, and mixed antibiotic (1:1) solutions were prepared with a concentration of 20 mg/L. Reactions were run in a batch test at two different pH values: 6 and 9. Aliquots were

TABLE 2 Variables used in the study.

Variable	Change in values
pH	6 and 9
Temperature	25°C and 40°C
Amount of Fe-modified biochar	0.1 g and 0.2 g

drawn from each flask at 0 min, 30 min, 60 min, 90 min, 120 min, 150 min, and 180 min, syringe-filtered, and measured using a UV-visible spectrophotometer.

2.5.1.2 Effect of Fe-modified biochar dose on antibiotic removal

Solutions of 20 mg/L of ciprofloxacin, azithromycin, and the mixture were prepared and run in a batch test at two different concentrations of Fe-modified biochar: 0.1 and 0.2 g. Aliquots were withdrawn after 0 min, 30 min, 60 min, 90 min, 120 min, 150 min, and 180 min, filtered, and subjected to a UV-visible spectrophotometer.

2.5.1.3 Effect of temperature on antibiotic removal

To determine the effect of temperature on antibiotic removal, solutions of 20 mg/L of ciprofloxacin, azithromycin, and mixture were prepared and run in a batch test at two temperatures, namely, 25 C and 40 C, with a 0.1 g adsorbent dose. Aliquots were withdrawn after 0 min, 30 min, 60 min, 90 min, 120 min, 150 min, and 180 min and syringe-filtered. After filtration, the absorbance values were measured using a UV-visible spectrophotometer. Variables used in the study are summarized in Table 2.

To understand the adsorption kinetics of the process and to evaluate adsorption mechanisms, pseudo-first-order and pseudo-second-order adsorption kinetic models were applied, analyzed, and calculated for ciprofloxacin, azithromycin, and the mixture of antibiotic uptake by Fe-modified biochar. Each experiment was conducted in duplicate, and the data underwent statistical analysis through the calculation of the arithmetic mean $\bar{x} = (\sum fx/n)$ and standard deviation $[\sigma = \sqrt{(\Sigma(xi - \mu)^2/N)}]$. Microsoft Excel and Origin were employed for data analysis and graph plotting.

3 Results

3.1 Yield of biochar and Fe-modified biochar

The yield of biochar obtained was 23.53%. The yield of biochar is influenced by two key factors: pyrolysis temperature and time. There is an inverse relationship between temperature and biochar yield, where an increase in temperature leads to a decrease in biochar yield. This correlation occurs due to processes like aromatization, dehydrogenation, decarboxylation, deoxygenation, and dehydration at higher temperatures, enhancing the carbonization process (Tomczyk et al., 2020). Likewise, extending the duration of pyrolysis results in increased evaporation of volatile components, thereby reducing the overall yield. Pine cones are a lignocellulosic biomass that contains abundant lignin, hemicellulose, and cellulose. During pyrolysis, the process of carbonization affects the lignin by decreasing hydrogen and oxygen content, releasing volatile organic compounds and carbon dioxide (Dawood et al., 2017). Rising temperatures induce the transformation of O-alkyl C into aryl and O-aryl furan-like structures, known for their high chemical reactivity (Yang et al., 2019). The pectin and lignin components were reduced by increasing the pyrolysis temperature, as verified by the FT-IR spectra. Pyrolysis at high temperatures shows biochar yields in the range of 20%–30% (Le et al., 2021) due to high ash content (Kaya and Uzun, 2021). Biochar conversion into iron-loaded biochar gave a yield of 80% (not 100%). The reduction in yield can be attributed to the loss of biochar during the process of chemical coprecipitation.

3.2 Characterization

3.2.1 FT-IR analysis

An FT-IR analysis was performed to observe surface functional groups on the obtained biochar. Both biochar and Fe-modified biochar showed similar spectral peaks with a variation in the intensity of peaks (Figure 1). The presence of bands in the spectral range of 775 cm^{-1} is because of aromatic (C–H) stretching (Song et al., 2019). The band at 1,433 cm^{-1} is assigned to (C–H) stretching (Wu et al., 2015). The peak in the region of 1,620 cm^{-1} is attributed to conjugated ketone C=O groups (Janu et al., 2021). The peak in the spectral region of 2,265 cm^{-1} is related to deformation vibrations or carbon dioxide in the C≡C plane (Zou et al., 2020). The peak at 3,075 cm^{-1} indicated the presence of aliphatic C-H folding (Wu et al., 2015). Lastly, a peak in the 3,632 cm^{-1} region signifies the presence of OH alcoholic and phenolic stretching. (Yi et al., 2020; Janu et al., 2021; Guel-Nájar et al., 2023). Moreover, the appearance of the band at approximately 529–552 cm^{-1} in Fe-modified biochar could be assigned to the stretching of the (Fe-O) vibration, showing it to be a magnetized material (Burbano et al., 2023).

3.2.2 X-ray diffraction

The crystalline structures of the biochar and Fe-modified biochar were characterized by X-ray diffraction (Figure 2). The appearance of the sharp peaks confirms the materials to be crystalline in nature. Strong peaks were observed at $2\theta = 26.5°$, 27.31° depicting the presence of graphite in biochar and Fe-modified biochar. In biochar and Fe-modified biochar, a peak at 31.9° and 50.8 due to silicon oxide (SiO_2) can be observed, respectively (Din et al., 2021a). SiO_2 is a compound that is prominent in the inorganic components of plant-based organic biomass (Guel-Nájar et al., 2023). It has been reported that pine trees have approximately 0.08–1.37 wt% of dry-weight silica in the needles and cones, depending on their family (Assefi et al., 2015). This silica can be found in biochar as the inorganic elements present in the biomass were not carbonized during pyrolysis. A study also concluded that biogenic Si was exposed under thermal treatment and migrated out of cell walls and onto the surface of grasses under thermal treatment (Pace et al., 2018). In the FT-IR analysis, SiO_2 typically exhibits a distinct sharp peak at 461 cm^{-1} (Zhao and Han, 2016). This could explain why this mineral was not detected by FT-IR, as the FT-IR spectra of both biochar and iron-modified biochar were recorded in the 4,000 to 550 cm^{-1} wavelength range. In the biochar sample, the peaks observed at 24.73° and 39.5 are indicative

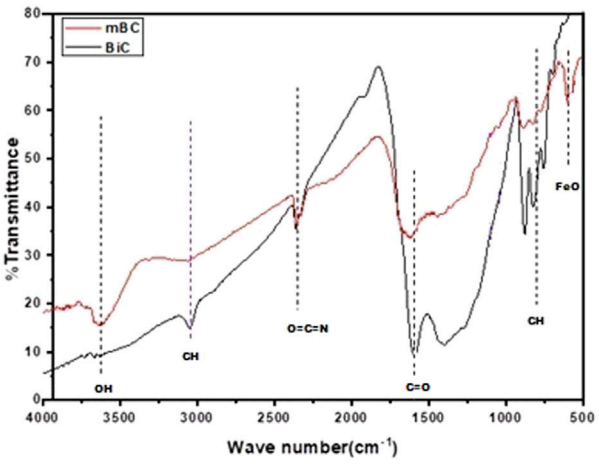

FIGURE 1
FT-IR spectra of biochar and magnetic biochar.

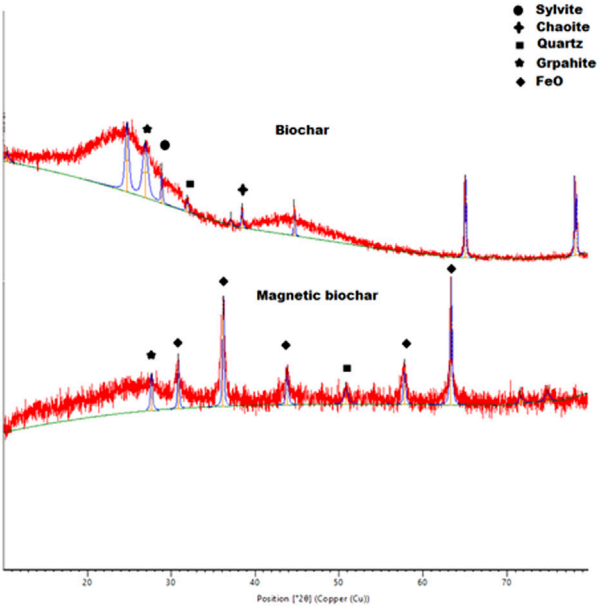

FIGURE 2
XRD spectra of biochar and magnetic biochar.

of the presence of carbon nanotubes and chaoite (Mopoung, 2015). Additionally, the relatively stronger peak at 28.87° suggests the presence of sylvite (KCl) (Pariyar et al., 2020), as potassium is the most abundant cation in plant cells (Dreyer and Uozumi, 2011). The diffraction peaks in the Fe-modified biochar sample appeared at 2θ = 30.80°, 35.80°, 43.80°, 54.2°, 57.77°, and 63.31°, indicating the presence of iron oxide (FeO) making biochar Fe-modified in nature (Din et al., 2021a).

3.2.3 Scanning electron microscopy

The SEM analysis of the biochar sample revealed a porous structure with cracks and irregularly distributed gaps on the biochar surface (Figure 3A). The biochar exhibited a fragmented structure characterized by cylindrical cavities and cracks (Claoston et al., 2014). Pores contribute to the biochar's overall surface area and create molecular sites capable of adsorption. Upon loading the biochar with $FeCl_3$ and $FeSO_4$, the surface of the modified biochar displayed increased roughness compared to the raw biochar (Figure 3B). The Fe-modified biochar showed a more heterogeneous structure, and a significant number of iron particles were observed to adhere to the material's surface, with some pores filled. Iron modification of biochar exerted a pronounced influence on the surface morphology of the material, leading to the dispersion of iron particles on the carbon matrix, consequently enhancing the specific surface area (Liu et al., 2015). The SEM image of the Fe-modified biochar clearly depicts the presence of particles immobilized on the surface, exhibiting a plate-like roughness and distorted morphology characterized by sharp edges and corners, as illustrated in the figure, in contrast to the regular appearance of the biochar (Din et al., 2021b).

3.3 Adsorption of antibiotics by Fe-modified biochar

The elimination of azithromycin, ciprofloxacin, and a mixture of antibiotics was calculated by the following formula Eq. (3) (Egbosiuba et al., 2020):

$$\%E = \frac{C_o - C_e}{C_o} \times 100. \quad (3)$$

The amount of antibiotic eliminated by Fe-modified biochar at equilibrium was determined by the following formula Eq. (4):

$$q_e = \frac{C_o - C_e}{W/V}, \quad (4)$$

where C_o and C_e are the initial and final antibiotic concentrations, respectively. V is the antibiotic solution volume in liters, and W is the mass of biochar in grams.

3.3.1 pH effect on the removal of antibiotics

To evaluate the impact of pH on the removal of antibiotics, the adsorption process was performed under pH 6 and pH 9. The removal percentages of azithromycin, ciprofloxacin, and the mixture at pH 6 were 80.1%, 87.3%, and 75.5%, respectively (Figure 4A). The removal percentages at pH 9 were 71.1%, 62.3%, and 68.3%, respectively (Figure 4B), suggesting pH 6 is more favorable for antibiotic removal from solution.

The qt versus t graph showed the maximum adsorption of antibiotics at 30–60 min. Then, the line flattens, depicting adsorption stopped after 120 min (Figure 5).

The absorption of antibiotics is influenced by pH due to the pH-dependent nature of their surface charge. As highlighted in Vasudevan et al. (2009), at a pH of 6, antibiotics predominantly exist in their cationic form. Concurrently, research by Ahmad et al. (2014) indicates that the Fe-modified biochar surface tends to carry a negative charge. This polarity difference potentially fosters electrostatic attraction between the negatively charged biochar surface and the cationic forms of antibiotics like azithromycin and ciprofloxacin, leading to increased sorption levels. At a

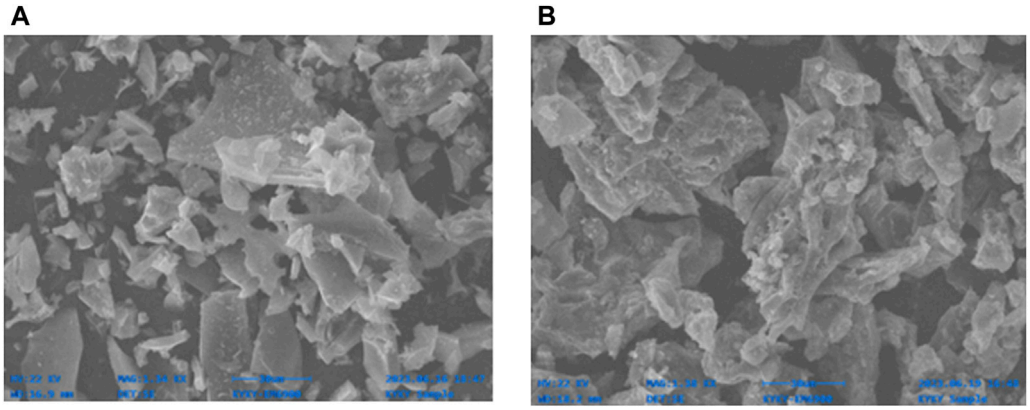

FIGURE 3
SEM image of **(A)** biochar and **(B)** Fe-modified biochar.

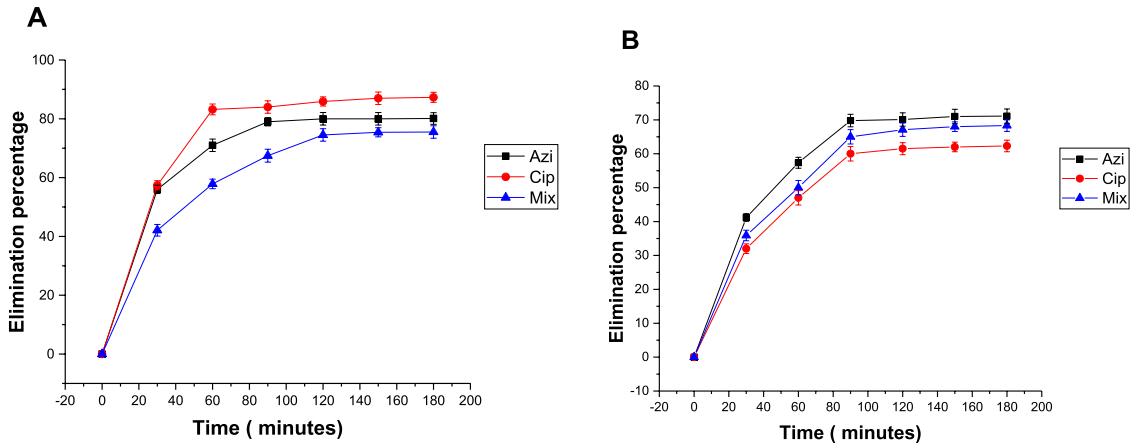

FIGURE 4
Effect of pH on the elimination percentage of antibiotics: **(A)** pH 6 and **(B)** pH 9.

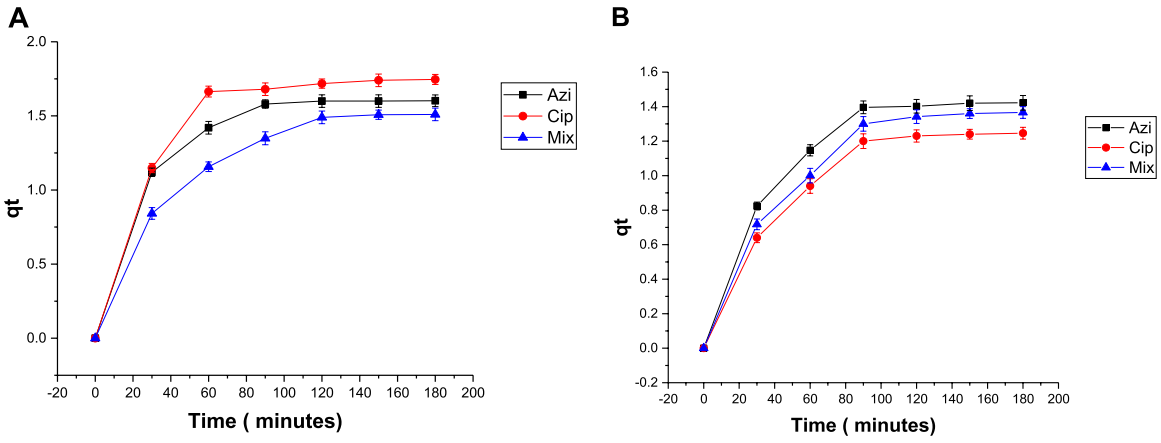

FIGURE 5
Plot of qt versus t at **(A)** pH 6 and **(B)** pH 9.

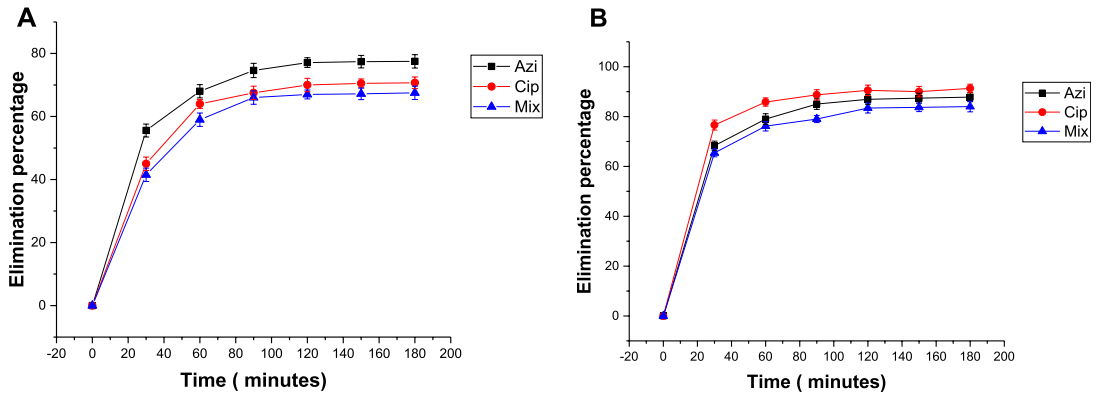

FIGURE 6
Effect of temperature on the elimination percentage of antibiotics: **(A)** 25°C and **(B)** 40°C.

pH of 9, the prevailing form of antibiotics shifts to the anionic state, leading to a significant decrease in the qe values. This decline stems from the electrostatic repulsion between the negatively charged Fe-modified biochar and the anionic antibiotics. Similar patterns emerged in the removal of ciprofloxacin from aqueous solutions using natural clay montmorillonite. At higher pH levels, ciprofloxacin gains a negative charge due to the deprotonation of its dicarboxylic group (Nassar et al., 2019). Conversely, at lower pH levels, ciprofloxacin molecules become positively charged owing to the protonation of the amine group (Roca Jalil et al., 2015). The molecular form of antibiotics can more easily interact with the surface of Fe-modified biochar, leading to increased adsorption (Shearer et al., 2022). In addition, ciprofloxacin and azithromycin have hydrophobic regions in their structures. At low pH, the Fe-modified biochar surface can become more hydrophobic due to changes in the protonation state of functional groups (Hassan et al., 2022). This increased hydrophobicity promotes the attraction between the antibiotics and the biochar surface through hydrophobic interactions, contributing to their higher adsorption.

3.3.2 Effect of temperature on the removal of antibiotics

To estimate the impact of temperature on antibiotic removal, adsorption was done at 25°C and 40°C. The elimination percentages of azithromycin, ciprofloxacin, and the mixture at 25°C were 77.5%, 70.7%, and 67.5%, respectively (Figure 6A). The elimination percentages at 40°C were 87.8%, 91.3%, and 84%, respectively (Figure 6B). Readings show that 40°C was the more favorable temperature for antibiotic removal.

The qt versus t graph showed maximum adsorption of antibiotics in the first hour, and then the graph gradually attained a linear pattern depicting adsorption reaching an equilibrium (Figure 7).

The rise in adsorption capacity as temperature increases indicates the endothermic nature of the adsorption process. This behavior predominantly arises from a synergy between physical and chemical adsorption mechanisms (Bhattacharyya et al., 2018). The rise in temperature increased the number of active sites on the Fe-modified biochar as well as its porosity and overall pore volume, which improved the surface's ability to bind antibiotics and, as a result, enhanced the adsorption process (Ge et al., 2023). In most studies, as the temperature rises, the solubility of antibiotics tends to decrease, consequently leading to an increase in adsorption (Aoulad et al., 2023). Additionally, the increase in temperature increases the molecular motion and entropy of the substance in the solution, thereby increasing the collision frequency between antibiotic molecules and functional groups present on the surface of Fe-modified biochar, augmenting the adsorption process (Li et al., 2014). Studies have demonstrated that as the temperature rises, the diffusion rate of antibiotics into both the external surface and internal pores of Fe-modified biochar particles significantly increases due to the increase in adsorbent sites owing to bond breakage at edges and the increased kinetic energy of antibiotic molecules that enhances their mobility, facilitating increased diffusion into the pores located on the surface of Fe-modified biochar (Behera et al., 2008; Zhou et al., 2019; Huang et al., 2021; Zhang et al., 2023).

3.3.3 Effect of Fe-modified biochar dose on the removal of antibiotics

As the adsorbent dosage rises, the removal of antibiotics increases. However, an excessive amount of adsorbent reaches a saturation point where adsorption and desorption achieve equilibrium, stalling further improvements in removal efficiency. This occurs because the active adsorption sites and functional groups become limited and unavailable (Amin et al., 2018).

To measure the effect of biochar dose on antibiotic removal, 0.1 g and 0.2 g samples of Fe-modified biochar were used. The elimination percentages of azithromycin, ciprofloxacin, and the mixture were 85.7%, 78%, and 82.6%, respectively, when using 0.1 g Fe-modified biochar (Figure 8A). The elimination percentages when using 0.2 g Fe-modified biochar were 76.4%, 72%, and 73.6%, respectively (Figure 8B). Elimination of azithromycin, ciprofloxacin, and the mixture from the solution was a maximum at the low Fe-modified biochar dosage. The qt versus time graph shows a similar pattern; maximum adsorption takes place within the first 30–60 min, and then, the line flattens, depicting adsorption stopped after 120 min (Figure 9).

The effect of Fe-modified biochar dosage was observed for removal efficiency and adsorption capacity of antibiotics, and it

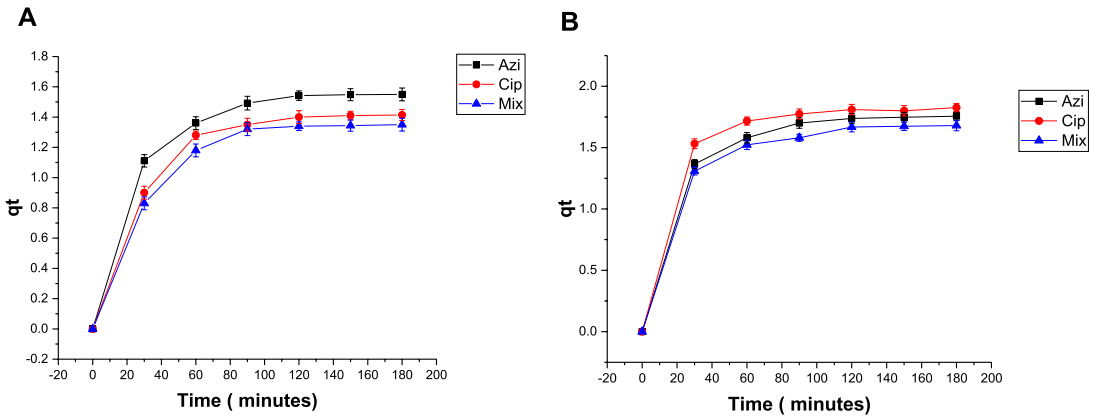

FIGURE 7
Plot of qt versus t at **(A)** 25°C and **(B)** 40°C.

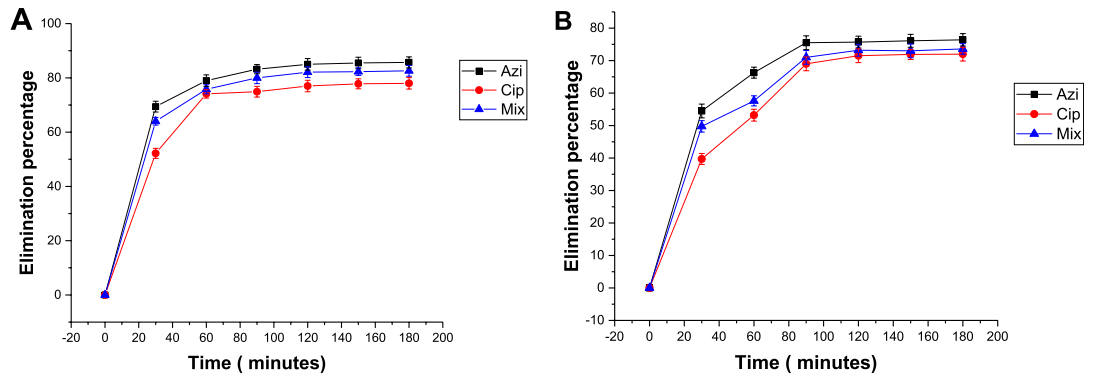

FIGURE 8
Effect of Fe-modified biochar dose on the elimination percentage of antibiotics: **(A)** 0.1 g Fe-modified biochar and **(B)** 0.2 g Fe-modified biochar.

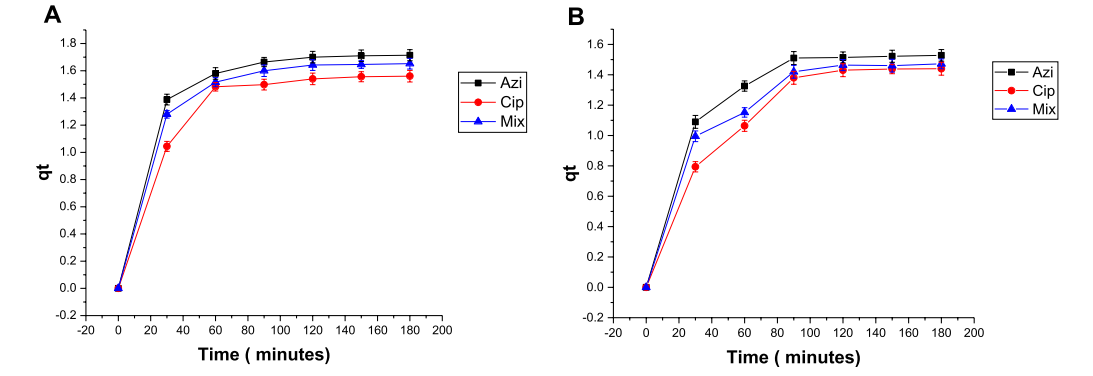

FIGURE 9
Plot of qt versus t with antibiotics: **(A)** 0.1 g Fe-modified biochar and **(B)** 0.2 g Fe-modified biochar.

was found that the adsorption capacity of antibiotics (qe) decreased with increasing Fe-modified biochar dosage. The reduction in removal efficiency might be attributed to an equilibrium point reached between the adsorption and desorption of antibiotics when an excessive amount of adsorbent was employed. At this stage, the removal efficiency plateaus due to the saturation of active adsorption sites and functional groups, limiting further removal (Amin et al., 2018). Because there are more potential binding sites per unit volume at low Fe-modified biochar concentrations, it is more likely that more antibiotic molecules will be adsorbed

TABLE 3 Kinetic parameters of a pseudo-first-order model for adsorption of antibiotics.

Pseudo-first-order model				
Amount of Fe-modified biochar	Parameter	Ciprofloxacin	Azithromycin	Mixture
0.1 g Fe-modified biochar	Q_e (mg/g)	1.57	1.72	1.66
	K_1 (min^{-1})	−0.01215 ± 0.00124	−0.0134 ± 9.18356E-4	−0.01276 ± 0.00109
	R^2 value	0.95021	0.97707	0.96491
0.2 g Fe-modified biochar	Q_e (mg/g)	1.45	1.53	1.48
	K_1 (min^{-1})	−0.01339 ± 0.00125	−0.01576 ± 0.00128	−0.01296 ± 0.00133
	R^2 value	0.95798	0.96829	0.94999

(Islam et al., 2021). High levels of Fe-modified biochar can cause the accessible binding sites to soon reach saturation. Because of this saturation, fewer antibiotic binding sites are available, which lowers the rate of adsorption (Sun et al., 2021). The competition for binding sites is lessened at low Fe-modified biochar concentrations due to the increased size of the available sorption surface (Ahmad et al., 2014; L. Liang et al., 2021), allowing a higher proportion of antibiotics to be adsorbed (Zou et al., 2022).

3.4 Adsorption kinetics

The kinetic adsorption mechanism process was studied by applying a pseudo-first-order model, a pseudo-second-order model, and an Elovich kinetic model for data analysis. The pseudo-first-order and pseudo-second-order models were created using linear equations (Alex Mbachu et al., 2023). The pseudo-first-order model asserts that the rate of adsorption of an adsorbate onto any adsorbent is directly related to the number of active sites present on the adsorbent. Pseudo-second-order kinetics emerge as a consequence of chemisorption phenomena during the adsorption process. The Elovich model is often used to explain chemical adsorption in which the rate of adsorption of solute decreases exponentially as the amount of adsorbed solute increases (Arif et al., 2023).

The pseudo-first-order model is expressed mathematically as Eq. (5)

$$log\,(Q_e - Q_t) = log\,(Q_l - \left(\frac{k_1}{20303}\right)t. \quad (5)$$

The pseudo-second-order model is shown as follows Eq. (6):

$$\frac{t}{Q_t} = \frac{1}{k_2\,(Qe)^2} + \frac{t}{Qe}. \quad (6)$$

The Elovich kinetic model is presented as follows Eq. (7):

$$Q_t = \frac{1}{\beta}\,ln(1 + a\,\beta\,t), \quad (7)$$

where:

- Qe is the equilibrium adsorption capacity (amount of solute adsorbed at equilibrium),
- Qt is the amount of solute adsorbed at time t,
- k_1 is the rate constant for the pseudo-first-order adsorption process,
- k_2 is the rate constant for the pseudo-second-order adsorption process,
- *a* is the rate constant for the Elovich kinetic model,
- β is the Elovich extent of surface coverage and activation energy of chemisorption, and
- t represents the time.

3.4.1 Pseudo-first-order model

The pseudo-first-order equation assumed that the rate of adsorption is directly proportional to the difference between the equilibrium adsorption capacity and the adsorption at a given time. R^2 values close to 1 indicate that the reaction is more inclined toward physisorption (Table 3).

R^2 values for azithromycin, ciprofloxacin, and the mixture at the 0.1 g Fe-modified biochar dose were 0.97707, 0.95021, and 0.96491, respectively. R^2 values for azithromycin, ciprofloxacin, and the mixture at the 0.2 g Fe-modified biochar dose were 0.96829, 0.95798, and 0.94999, respectively (Figures 10A, B). The fact that none of the R^2 values reached 0.99 indicates that adsorption kinetics data did not perfectly follow the pseudo-first-order kinetic model.

3.4.2 Pseudo-second-order model

The pseudo-second-order equation assumed that the rate of adsorption is proportional to the square of the difference between the equilibrium adsorption capacity and the adsorption at a given time, and it followed second-order kinetics. A pseudo-second-order reaction is more inclined toward chemisorption.

R^2 values for azithromycin, ciprofloxacin, and the mixture at the 0.1 g Fe-modified biochar dose were 0.99853, 0.99434, and 0.99789, respectively. R^2 values for azithromycin, ciprofloxacin, and the mixture at the 0.2 g Fe-modified biochar dose were 0.9950, 0.97579, and 0.9892, respectively (Figures 11A, B; Table 4). As R^2 values of the pseudo-second-order reaction are closer to 1 than the R^2 values of the pseudo-first-order reaction, it can be assumed that adsorption kinetic data for both antibiotics and their mixture are more inclined toward and kinetically controlled as a pseudo-second-order reaction representing chemisorption (Aoulad et al., 2023), including various mechanisms, such as ion exchange and electrostatic interaction (Nasiri Azad et al., 2015).

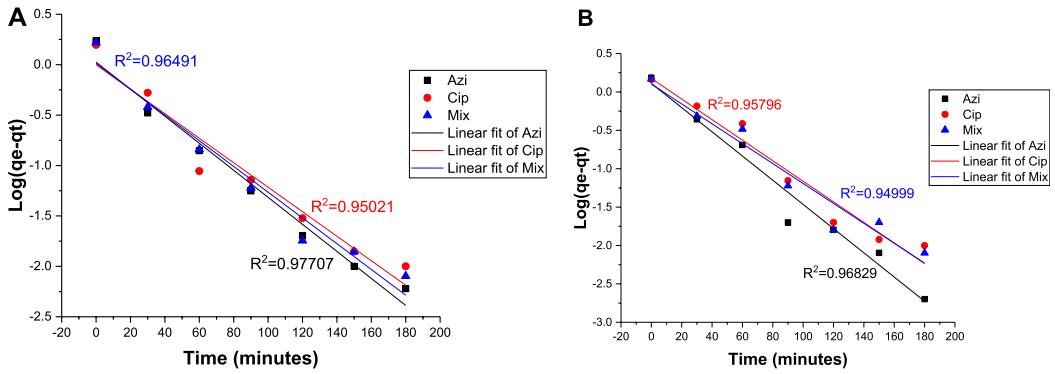

FIGURE 10
Pseudo-first-order model: **(A)** 0.10 g Fe-modified biochar and **(B)** 0.20 g Fe-modified biochar.

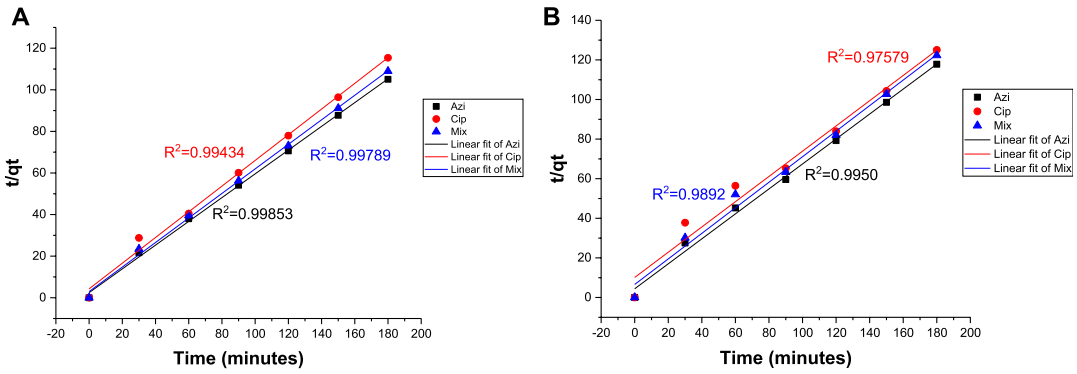

FIGURE 11
Pseudo-second-order model: **(A)** 0.10 g Fe-modified biochar and **(B)** 0.20 g Fe-modified biochar.

TABLE 4 Kinetic parameters of a pseudo-second-order model for the adsorption of antibiotics.

Pseudo-second-order model				
Amount of Fe-modified biochar	Parameter	Ciprofloxacin	Azithromycin	Mixture
0.1 g Fe-modified biochar	Q_e (mg/g)	1.57	1.72	1.66
	K_2 (mg g^{-1} min^{-1})	0.61775 ± 0.02084	0.57128 ± 0.00981	0.5902 ± 0.01215
	R^2 value	0.99434	0.99853	0.99789
0.2 g Fe-modified biochar	Q_e (mg/g)	1.45	1.53	1.48
	K_2 (min^{-1})	0.6376 ± 0.04492	0.63033 ± 0.0198	0.64513 ± 0.03001
	R^2 value	0.97579	0.9950	0.9892

These findings are consistent with the findings of the pH experiment.

3.4.3 Elovich kinetic model

The Elovich model is applied to understand the chemisorption nature of adsorption. The Elovich model suggests that adsorption occurs through a multistep process, and the rate of adsorption is not constant but decreases with time due to the decreasing number of available active sites on the adsorbent surface. The graph of qt versus lnt helps determine the nature of adsorption on the heterogeneous surface of the adsorbent, whether chemisorption or not (Abdu et al., 2021). R^2 values for azithromycin, ciprofloxacin, and the mixture at a 0.1 g Fe-modified biochar dose were 0.93629, 0.97983, and 0.98033, respectively. R^2 values for azithromycin, ciprofloxacin, and the mixture at a 0.2 g Fe-modified biochar dose were 0.97286, 0.94579, and 0.97311,

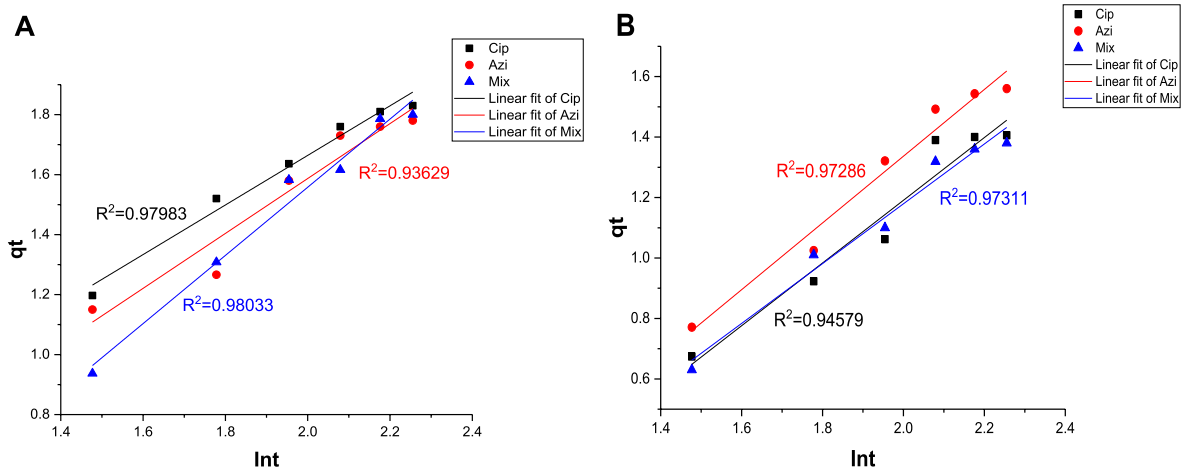

FIGURE 12
Elovich kinetic model: **(A)** 0.10 g Fe-modified biochar and **(B)** 0.20 g Fe-modified biochar.

TABLE 5 Kinetic parameters of the Elovich model for the adsorption of antibiotics.

Elovich kinetic model				
Amount of Fe-modified biochar	Parameter	Ciprofloxacin	Azithromycin	Mixture
0.1 g Fe-modified biochar	Q_e (mg/g)	1.57	1.72	1.66
	a (g/mg/min²)	1.230739	1.103424	0.888849
	β (mg/g/min)	0.013218	−0.26724	−0.6111
	R^2 value	0.97983	0.93629	0.98033
0.2 g Fe-modified biochar	Q_e (mg/g)	1.45	1.53	1.48
	a (g/mg/min²)	0.99995	0.941132	1.032237
	β (mg/g/min)	−0.87498	−0.7941	−0.80646
	R^2 value	0.94579	0.97286	0.97311

respectively (Figures 12A, B; Table 5). Relatively higher R^2 values showed an Elovich fit, indicating the establishment of chemical interactions of antibiotics with the functional groups present in biochar. The Elovich model is often used to explain chemical adsorption in which the rate decreases with time as the surface area of the adsorbed substance increases.

Comparing the R^2 values for the pseudo-first-order, pseudo-second-order, and Elovich kinetic models for antibiotic adsorption onto Fe-modified biochar, it was observed that pseudo-second-order kinetic was the model with the best fit, and the adsorption kinetic data align more closely with the pseudo-second-order model, which signifies a form of chemisorption (Aoulad et al., 2023). Previous studies linked the applicability of the pseudo-second-order model to the chemisorption mechanism supporting the presence of multiple adsorption sites (Abdu et al., 2021). However, Baraka (2012) suggested that adsorption data that follow a pseudo-second-order kinetic model could be an indication of both chemisorption and physical adsorption mechanisms. Chemical adsorption mechanisms include ion exchange, complexation, and electrostatic interaction (Nasiri Azad et al., 2015; Ambaye et al., 2021). During the iron loading onto biochar, chemical modifications can occur through the addition of iron salts. These modifications introduce functional groups that contribute to enhanced electrostatic interactions, hydrogen bonding, and π–π stacking interactions with antibiotics, promoting their adsorption onto the surface of the modified biochar (Xu et al., 2022).

Fe-modified biochar generally implies electrostatic interaction as the adsorption mechanism for the removal of organic pollutants from water (Abbas et al., 2018). However, experimental conditions also determine the type of forces involved in adsorption processes; that is, the strength and nature of the electrostatic force depend on the solution pH. The functional groups found on the surface of Fe-modified biochar facilitate the chemical bonding between positively charged antibiotics and negatively charged modified biochar (Kumari et al., 2020). Adding iron sulfate to biochar decreases biochar flammability while increasing the recalcitrant carbon fraction and content of oxygen-containing functional groups on the surface of biochar (Pace et al., 2018). The adsorption of antibiotics onto the Fe-modified biochar surface is a multi-faceted process, encompassing diverse mechanisms like ion

exchange, complexation, precipitation, electrostatic interaction, physical adsorption involving pore filling, and complexation reactions associated with surface functional groups, such as FeO (Jiang et al., 2023; Liang et al., 2022). The adsorption processes may also include other interactions, including hydrogen bonds, π–π stacking, and van der Waals forces (Li et al., 2018; Song et al., 2019). In one study, tetracyclines exhibited high adsorption efficiency onto Fe-modified biochar derived from rice waste, attributed to the synergy of pore filling, electrostatic attraction, π–π interactions, and the complexation reactions of surface functional groups (Zhang et al., 2023). The particular reactions taking place during the adsorption process can differ based on various factors like the properties of the iron-modified biochar, environmental circumstances, and the nature of the pollutants being adsorbed (Zou et al., 2022).

4 Conclusion

The study investigated the removal of antibiotics from an aqueous solution utilizing Fe-modified biochar derived from pine cones. Characterization of Fe-modified biochar suggested that it is crystalline in nature and rich in minerals, functional groups, and Fe-O, causing it to be adsorptive in nature owing to its increased surface area, iron modification, and synergistic effects. Maximum removal percentages of azithromycin, ciprofloxacin, and their mixture were 88%, 90%, and 85%, respectively. The optimum conditions for maximum elimination of antibiotics were pH 6, 40 C temperature, and 0.1 g dose of Fe-modified biochar. An increase in temperature and low pH was found to increase the removal efficiency of azithromycin, ciprofloxacin, and the mixture of both antibiotics. The adsorption process was found to obey a pseudo-second-order kinetic model, indicating a chemical sorption mechanism. Current findings suggest that Fe-modified biochar has great potential for removing antibiotics from aqueous environments. In addition, the conversion of pine cones into Fe-modified biochar is a valuable strategy for waste reduction by transforming the former into an adsorbent, offering a promising approach for water treatment and pollution remediation.

Data availability statement

The raw data supporting the conclusion of this article will be made available by the authors, without undue reservation.

Author contributions

SaA: conceptualization, data curation, formal analysis, investigation, writing–original draft, writing–review and editing, methodology, project administration, supervision, and validation. SuA: data curation, formal analysis, investigation, methodology, and writing–original draft. II: formal analysis, methodology, and writing–review and editing. TF: formal analysis, methodology, writing–review and editing, and data curation. AI: data curation, formal analysis, methodology, and writing–review and editing. LA: data curation, formal analysis, writing–review and editing, conceptualization, investigation, and writing–original draft.

Funding

The authors declare that no financial support was received for the research, authorship, and/or publication of this article.

Conflict of interest

The authors declare that the research was conducted in the absence of any commercial or financial relationships that could be construed as a potential conflict of interest.

Publisher's note

All claims expressed in this article are solely those of the authors and do not necessarily represent those of their affiliated organizations, or those of the publisher, the editors, and the reviewers. Any product that may be evaluated in this article, or claim that may be made by its manufacturer, is not guaranteed or endorsed by the publisher.

References

Abbas, Z., Ali, S., Rizwan, M., Zaheer, I. E., Malik, A., Riaz, M. A., et al. (2018). A critical review of mechanisms involved in the adsorption of organic and inorganic contaminants through biochar. *Arabian J. Geosciences* 11 (16), 448. doi:10.1007/s12517-018-3790-1

Abdu, N., Yusuf, A. A., Mukhtar, B., and Solomon, R. I. (2021). Kinetics and thermodynamics of nitrate adsorption by biochar. *EQA-International J. Environ. Qual.* 41, 17–32. doi:10.6092/issn.2281-4485/10481

Ahmad, M., Rajapaksha, A. U., Lim, J. E., Zhang, M., Bolan, N., Mohan, D., et al. (2014). Biochar as a sorbent for contaminant management in soil and water: a review. *Chemosphere* 99, 19–33. doi:10.1016/j.chemosphere.2013.10.071

Alex Mbachu, C., Kamoru Babayemi, A., Chinedu Egbosiuba, T., Ifeanyichukwu Ike, J., Jacinta Ani, I., and Mustapha, S. (2023). Green synthesis of iron oxide nanoparticles by Taguchi design of experiment method for effective adsorption of methylene blue and methyl orange from textile wastewater. *Results Eng.* 19 (May), 101198. doi:10.1016/j.rineng.2023.101198

Ambaye, T. G., Vaccari, M., van Hullebusch, E. D., Amrane, A., and Rtimi, S. (2021). Mechanisms and adsorption capacities of biochar for the removal of organic and inorganic pollutants from industrial wastewater. *Int. J. Environ. Sci. Technol.* 18 (10), 3273–3294. doi:10.1007/s13762-020-03060-w

Amin, M. T., Alazba, A. A., and Shafiq, M. (2018). Removal of copper and lead using banana biochar in batch adsorption systems: isotherms and kinetic studies. *Arabian J. Sci. Eng.* 43 (11), 5711–5722. doi:10.1007/s13369-017-2934-z

Aoulad, Y., Hadj, E., Mohammadi, A., Ait, A., and Youness, L. (2023). Recent advances and prospects of biochar - based adsorbents for malachite green removal: a comprehensive review. *Chem. Afr.* 6 (2), 579–608. doi:10.1007/s42250-022-00391-8

Arif, M., Liu, G., Zia ur Rehman, M., Mian, M. M., Ashraf, A., Yousaf, B., et al. (2023). Impregnation of biochar with montmorillonite and its activation for the removal of azithromycin from aqueous media. *Environ. Sci. Pollut. Res.* 30 (32), 78279–78293. doi:10.1007/s11356-023-27908-z

Asadi-Ghalhari, M., Kishipour, A., sadat Tabatabaei, F., and Mostafaloo, R. (2022). Ciprofloxacin removal from aqueous solutions by granular ferric hydroxide: modeling and optimization. *J. Trace Elem. Minerals* 2 (June), 100007. doi:10.1016/j.jtemin.2022.100007

Assefi, M., Davar, F., and Hadadzadeh, H. (2015). Green synthesis of nanosilica by thermal decomposition of pine cones and pine needles. *Adv. Powder Technol.* 26 (6), 1583–1589. doi:10.1016/j.apt.2015.09.004

Balarak, D., Khatibi, A. D., and Chandrika, K. (2020). Antibiotics removal from aqueous solution and pharmaceutical wastewater by adsorption process: a review. *Int. J. Pharm. Investigation* 10 (2), 106–111. doi:10.5530/ijpi.2020.2.19

Balarak, D., Mahvi, A. H., Shahbaksh, S., Wahab, M. A., and Abdala, A. (2021). Adsorptive removal of azithromycin antibiotic from aqueous solution by Azolla filiculoides-based activated porous carbon. *Nanomater. (Basel).* 11 (12), 3281. doi:10.3390/nano11123281

Baraka, A. (2012). Adsorptive removal of tartrazine and methylene blue from wastewater using melamine-formaldehyde-tartaric acid resin (and a discussion about pseudo second order model). *Desalination Water Treat.* 44 (1–3), 128–141. doi:10.1080/19443994.2012.691778

Behera, S. K., Kim, J. H., Guo, X., and Park, H. S. (2008). Adsorption equilibrium and kinetics of polyvinyl alcohol from aqueous solution on powdered activated carbon. *J. Hazard. Mater.* 153 (3), 1207–1214. doi:10.1016/j.jhazmat.2007.09.117

Bhandari, G., Gangola, S., Dhasmana, A., Rajput, V., Gupta, S., Malik, S., et al. (2023). Nano-biochar: recent progress, challenges, and opportunities for sustainable environmental remediation. *Front. Microbiol.* 14 (July), 1214870–1214916. doi:10.3389/fmicb.2023.1214870

Bhattacharyya, A., Banerjee, B., Ghorai, S., Rana, D., Roy, I., Sarkar, G., et al. (2018). Development of an auto-phase separable and reusable graphene oxide-potato starch based cross-linked bio-composite adsorbent for removal of methylene blue dye. *Int. J. Biol. Macromol.* 116, 1037–1048. doi:10.1016/j.ijbiomac.2018.05.069

Burbano, A. A., Gascó, G., Horst, F., Lassalle, V., and Méndez, A. (2023). Production, characteristics and use of magnetic biochar nanocomposites as sorbents. *Biomass Bioenergy* 172 (February), 106772. doi:10.1016/j.biombioe.2023.106772

Cela-Dablanca, R., Barreiro, A., Rodríguez-López, L., Pérez-Rodríguez, P., Arias-Estévez, M., Fernández-Sanjurjo, M. J., et al. (2022). Azithromycin adsorption onto different soils. *Processes* 10 (12), 2565–2610. doi:10.3390/pr10122565

Chandrasekaran, A., Patra, C., Narayanasamy, S., and Subbiah, S. (2020). Adsorptive removal of Ciprofloxacin and Amoxicillin from single and binary aqueous systems using acid-activated carbon from Prosopis juliflora. *Environ. Res.*, 188, 109825. doi:10.1016/j.envres.2020.109825

Chen, Z., Pei, J., Wei, Z., Ruan, X., Hua, Y., Xu, W., et al. (2021). A novel maize biochar-based compound fertilizer for immobilizing cadmium and improving soil quality and maize growth. *Environ. Pollut.* 277, 116455. doi:10.1016/j.envpol.2021.116455

Claoston, N., Samsuri, A. W., Ahmad Husni, M. H., and Mohd Amran, M. S. (2014). Effects of pyrolysis temperature on the physicochemical properties of empty fruit bunch and rice husk biochars. *Waste Manag. Res.* 32 (4), 331–339. doi:10.1177/0734242X14525822

Davoodi, S., Dahrazma, B., Goudarzi, N., and Gorji, H. G. (2019). Adsorptive removal of azithromycin from aqueous solutions using raw and saponin-modified nano diatomite. *Water Sci. Technol.* 80 (5), 939–949. doi:10.2166/wst.2019.337

Dawood, S., Sen, T. K., and Phan, C. (2017). Synthesis and characterization of slow pyrolysis pine cone bio-char in the removal of organic and inorganic pollutants from aqueous solution by adsorption: kinetic, equilibrium, mechanism and thermodynamic. *Bioresour. Technol.* 246, 76–81. doi:10.1016/j.biortech.2017.07.019

Din, S. U., Azeez, A., Zain-ul-Abdin, Haq, S., Hafeez, M., Imran, M., et al. (2021a). Investigation on cadmium ions removal from water by a nanomagnetite based biochar derived from Eleocharis dulcis. *J. Inorg. Organomet. Polym. Mater.* 31 (1), 415–425. doi:10.1007/s10904-020-01758-5

Din, S. U., Khan, M. S., Hussain, S., Imran, M., Haq, S., Hafeez, M., et al. (2021b). Adsorptive mechanism of chromium adsorption on siltstone–nanomagnetite–biochar composite. *J. Inorg. Organomet. Polym. Mater.* 31 (4), 1608–1620. doi:10.1007/s10904-020-01829-7

Ding, C., and He, J. (2010). Effect of antibiotics in the environment on microbial populations. *Applied Microbiology and Biotechnology*. 87. 925–941. doi:10.1007/s00253-010-2649-5

Dorgali, M. V., Longo, A., Vass, C., Shields, G., Harrison, R., and Boeri, M. (2020). PMU97 exploring antimicrobial resistance (AMR) from a societal perspective: preferences and welfare impacts in the United Kingdom. *Value Health* 23 (December), S619. doi:10.1016/j.jval.2020.08.1309

Dreyer, I., and Uozumi, N. (2011). Potassium channels in plant cells. *FEBS J.* 278 (22), 4293–4303. doi:10.1111/j.1742-4658.2011.08371.x

Egbosiuba, T. C. (2022). Biochar and bio-oil fuel properties from nickel nanoparticles assisted pyrolysis of cassava peel. *Heliyon* 8 (8), e10114. doi:10.1016/j.heliyon.2022.e10114

Egbosiuba, T. C., Abdulkareem, A. S., Kovo, A. S., Afolabi, E. A., Tijani, J. O., Auta, M., et al. (2020). Ultrasonic enhanced adsorption of methylene blue onto the optimized surface area of activated carbon: adsorption isotherm, kinetics and thermodynamics. *Chem. Eng. Res. Des.* 153, 315–336. doi:10.1016/j.cherd.2019.10.016

Gasim, M. F., Choong, Z. Y., Koo, P. L., Low, S. C., Abdurahman, M. H., Ho, Y. C., et al. (2022). Application of biochar as functional material for remediation of organic pollutants in water: an overview. *Catalysts* 12 (2), 210–226. doi:10.3390/catal12020210

Ge, Q., Li, P., Liu, M., Xiao, G., Ming, Z., Gai, X. K., et al. (2023). Removal of methylene blue by porous biochar obtained by KOH activation from bamboo biochar. *Bioresour. Bioprocess.* 10 (1), 51. doi:10.1186/s40643-023-00671-2

Guel-Nájar, N. A., Rios-Hurtado, J. C., Muzquiz-Ramos, E. M., Dávila-Pulido, G. I., González-Ibarra, A. A., and Pat-Espadas, A. M. (2023). Magnetic biochar obtained by chemical coprecipitation and pyrolysis of corn cob residues: characterization and methylene blue adsorption. *Materials* 16 (8), 3127. doi:10.3390/ma16083127

Hafeez, A., Pan, T., Tian, J., and Cai, K. (2022). Modified biochars and their effects on soil quality: a review. *Environ. - MDPI* 9 (5), 60. doi:10.3390/environments9050060

Han, Y., Cao, X., Ouyang, X., Sohi, S. P., and Chen, J. (2016). Adsorption kinetics of magnetic biochar derived from peanut hull on removal of Cr (VI) from aqueous solution: effects of production conditions and particle size. *Chemosphere* 145, 336–341. doi:10.1016/j.chemosphere.2015.11.050

Hassan, M., Du, J., Liu, Y., Naidu, R., Zhang, J., Ahsan, M. A., et al. (2022). Magnetic biochar for removal of perfluorooctane sulphonate (PFOS): interfacial interaction and adsorption mechanism. *Environ. Technol. Innovation* 28, 102593. doi:10.1016/j.eti.2022.102593

Huang, F., Zhang, S. M., Wu, R. R., Zhang, L., Wang, P., and Xiao, R. B. (2021). Magnetic biochars have lower adsorption but higher separation effectiveness for Cd2+ from aqueous solution compared to nonmagnetic biochars. *Environ. Pollut.* 275, 116485. doi:10.1016/j.envpol.2021.116485

Hussain, S., Ghouri, A. S., and Ahmad, A. (2019). Pine cone extract as natural coagulant for purification of turbid water. *Heliyon* 5 (3), e01420. doi:10.1016/j.heliyon.2019.e01420

Islam, T., Li, Y., and Cheng, H. (2021). Biochars and engineered biochars for water and soil remediation: a review. *Sustain. Switz.* 13 (17), 9932–10025. doi:10.3390/su13179932

Janu, R., Mrlik, V., Ribitsch, D., Hofman, J., Sedláček, P., Bielská, L., et al. (2021). Biochar surface functional groups as affected by biomass feedstock, biochar composition and pyrolysis temperature. *Carbon Resour. Convers.* 4 (January), 36–46. doi:10.1016/j.crcon.2021.01.003

Jiang, M., He, L., Niazi, N. K., Wang, H., Gustave, W., Vithanage, M., et al. (2023). Nanobiochar for the remediation of contaminated soil and water: challenges and opportunities. *Biochar* 5 (1), 2. doi:10.1007/s42773-022-00201-x

Kaya, N., and Uzun, Z. Y. (2021). Investigation of effectiveness of pine cone biochar activated with KOH for methyl orange adsorption and CO2 capture. *Biomass Convers. Biorefinery* 11 (3), 1067–1083. doi:10.1007/s13399-020-01063-8

Khokhar, T. S., Memon, F. N., Memon, A. A., Durmaz, F., Memon, S., Panhwar, Q. K., et al. (2019). Removal of ciprofloxacin from aqueous solution using wheat bran as adsorbent. *Sep. Sci. Technol.* 54 (8), 1278–1288. doi:10.1080/01496395.2018.1536150

Kovalakova, P., Cizmas, L., Mcdonald, T. J., and Marsalek, B. (2020). Occurrence and toxicity of antibiotics in the aquatic environment: a review. *Chemosphere*. 251. 126351. doi:10.1016/j.chemosphere.2020.126351

Kumari, S., Khan, A. A., Chowdhury, A., Bhakta, A. K., Mekhalif, Z., and Hussain, S. (2020). Efficient and highly selective adsorption of cationic dyes and removal of ciprofloxacin antibiotic by surface modified nickel sulfide nanomaterials: kinetics, isotherm and adsorption mechanism. *Colloids Surfaces A Physicochem. Eng. Aspects* 586, 124264. doi:10.1016/j.colsurfa.2019.124264

Kümmerer, K. (2003). Significance of antibiotics in the environment. *J. Antimicrob. Chemother.*, 52 5–7. doi:10.1093/jac/dkg293

Kümmerer, K. (2009). The presence of pharmaceuticals in the environment due to human use - present knowledge and future challenges. *J. Environ. Manag.* 90 (8), 2354–2366. doi:10.1016/j.jenvman.2009.01.023

Le, P. T., Bui, H. T., Le, D. N., Nguyen, T. H., Pham, L. A., Nguyen, H. N., et al. (2021). Preparation and characterization of biochar derived from agricultural by-products for dye removal. *Adsorpt. Sci. Technol.* 2021, 1–14. doi:10.1155/2021/9161904

Li, B., Wang, Q., Guo, J. Z., Huan, W. W., and Liu, L. (2018). Sorption of methyl orange from aqueous solution by protonated amine modified hydrochar. *Bioresour. Technol.* 268, 454–459. doi:10.1016/j.biortech.2018.08.023

Li, H., Zhang, D., Han, X., and Xing, B. (2014). Adsorption of antibiotic ciprofloxacin on carbon nanotubes: PH dependence and thermodynamics. *Chemosphere* 95, 150–155. doi:10.1016/j.chemosphere.2013.08.053

Li, X., Wang, C., Zhang, J., Liu, J., Liu, B., and Chen, G. (2020). Preparation and application of magnetic biochar in water treatment: a critical review. *Sci. Total Environ.* 711, 134847. doi:10.1016/j.scitotenv.2019.134847

Liang, H., Zhu, C., Ji, S., Kannan, P., and Chen, F. (2022). Magnetic Fe2O3/biochar composite prepared in a molten salt medium for antibiotic removal in water. *Biochar* 4 (1), 3–13. doi:10.1007/s42773-021-00130-1

Liang, L., Xi, F., Tan, W., Meng, X., Hu, B., and Wang, X. (2021). Review of organic and inorganic pollutants removal by biochar and biochar-based composites. *Biochar* 3 (3), 255–281. doi:10.1007/s42773-021-00101-6

Liu, F., Zuo, J., Chi, T., Wang, P., and Yang, B. (2015). Removing phosphorus from aqueous solutions by using iron-modified corn straw biochar. *Front. Environ. Sci. Eng.* 9 (6), 1066–1075. doi:10.1007/s11783-015-0769-y

Lu, L., Yu, W., Wang, Y., Zhang, K., Zhu, X., Zhang, Y., et al. (2020). Application of biochar-based materials in environmental remediation: from multi-level structures to specific devices. *Biochar* 2 (Issue 1), 1–31. doi:10.1007/s42773-020-00041-7

Ma, J., Yang, M., Yu, F., and Zheng, J. (2015). Water-enhanced removal of ciprofloxacin from water by porous graphene hydrogel. *Sci. Rep.* 5 (1), 13578. doi:10.1038/srep13578

Manaia, C. M. (2017). Assessing the risk of antibiotic resistance transmission from the environment to humans: non-direct proportionality between abundance and risk. *Trends Microbiol.* 25 (3), 173–181. doi:10.1016/j.tim.2016.11.014

Martõ, Â. L., Alonso, A., and Sa, P. (2001). *Minireview Environ. Sel. antibiotic Resist. Genes* 3, 1–9. doi:10.1046/j.1462-2920.2001.00161.x

Mirzaei, R., Yunesian, M., Nasseri, S., Gholami, M., Jalilzadeh, E., Shoeibi, S., et al. (2018). Occurrence and fate of most prescribed antibiotics in different water environments of Tehran, Iran. *Sci. Total Environ.* 619–620, 446–459. doi:10.1016/j.scitotenv.2017.07.272

Mirzaie, F., Teymori, F., Shahcheragh, S., and Dobaradaran, S. (2020). Occurrence and distribution of azithromycin in wastewater treatment plants, seawater, and sediments of the northern part of the Persian Gulf around Bushehr port: a comparison with Pre-COVID 19 pandemic. *Chemosphere*, 307. doi:10.1016/j.chemosphere.2022.135996

Mopoung, S. (2015). Occurrence of Carbon Nanotube from Banana Peel Activated Carbon Mixed with Occurrence of carbon nanotube from banana peel activated carbon mixed with mineral oil. *Int. J. Phys. Sci.* 6, 1789–1792. doi:10.5897/IJPS10.489

Nakahira, A., Nishida, S., and Fukunishi, K. (2006). Synthesis of magnetic activated carbons for removal of environmental endocrine disrupter using magnetic vector. *J. Ceram. Soc. Jpn.* 114 (1325), 135–137. doi:10.2109/jcersj.114.135

Nasiri Azad, F., Ghaedi, M., Dashtian, K., Hajati, S., Goudarzi, A., and Jamshidi, M. (2015). Enhanced simultaneous removal of malachite green and safranin O by ZnO nanorod-loaded activated carbon: modeling, optimization and adsorption isotherms. *New J. Chem.* 39 (10), 7998–8005. doi:10.1039/c5nj01281c

Nassar, M. Y., Ahmed, I. S., and Raya, M. A. (2019). A facile and tunable approach for synthesis of pure silica nanostructures from rice husk for the removal of ciprofloxacin drug from polluted aqueous solutions. *J. Mol. Liq.* 282, 251–263. doi:10.1016/j.molliq.2019.03.017

Nazraz, M., Yamini, Y., and Asiabi, H. (2019). Chitosan-based sorbent for efficient removal and extraction of ciprofloxacin and norfloxacin from aqueous solutions. *Microchim. Acta* 186 (7), 459. doi:10.1007/s00604-019-3563-x

Osińska, A., Korzeniewska, E., Harnisz, M., Felis, E., Bajkacz, S., Jachimowicz, P., et al. (2020). Small-scale wastewater treatment plants as a source of the dissemination of antibiotic resistance genes in the aquatic environment. *J. Hazard. Mater.* 381, 121221. doi:10.1016/j.jhazmat.2019.121221

Pace, B., Munroe, P., Marjo, C. E., Thomas, P., Gong, B., Shepherd, J., et al. (2018). The mechanisms and consequences of inorganic reactions during the production of ferrous sulphate enriched bamboo biochars. *J. Anal. Appl. Pyrolysis* 131, 101–112. doi:10.1016/j.jaap.2018.01.028

Pariyar, P., Kumari, K., Jain, M. K., and Jadhao, P. S. (2020). Evaluation of change in biochar properties derived from different feedstock and pyrolysis temperature for environmental and agricultural application. *Sci. Total Environ.* 713, 136433. doi:10.1016/j.scitotenv.2019.136433

Peñafiel, M. E., Vanegas, E., Bermejo, D., Matesanz, J. M., and Ormad, M. P. (2019). Organic residues as adsorbent for the removal of ciprofloxacin from aqueous solution. *Hyperfine Interact.* 240 (1), 71. doi:10.1007/s10751-019-1612-9

Phoon, B. L., Ong, C. C., Shuaib, M., Saheed, M., Show, P., Chang, J., et al. (2020). Conventional and emerging technologies for removal of antibiotics from wastewater. *J. Hazard. Mater.* 400, 122961. doi:10.1016/j.jhazmat.2020.122961

Roca Jalil, M. E., Baschini, M., and Sapag, K. (2015). Influence of pH and antibiotic solubility on the removal of ciprofloxacin from aqueous media using montmorillonite. *Appl. Clay Sci.* 114, 69–76. doi:10.1016/j.clay.2015.05.010

Sahin, H., and Yalcin, O. (2017). Conifer cones: an alternative raw material for industry. *Br. J. Pharm. Res.* 17 (2), 1–9. doi:10.9734/bjpr/2017/34153

Sanni, A., Alaya-ibrahim, S., Saka, A., David, O., Chinedu, T., Oladejo, J., et al. (2023). Column adsorption of biological oxygen demand, chemical oxygen demand and total organic carbon from wastewater by magnetite nanoparticles-zeolite A composite. *Heliyon* 9 (2), e13095. doi:10.1016/j.heliyon.2023.e13095

Sarkar, A., Ranjan, A., and Paul, B. (2019). Synthesis, characterization and application of surface-modified biochar synthesized from rice husk, an agro-industrial waste for the removal of hexavalent chromium from drinking water at near-neutral pH. *Clean Technol. Environ. Policy* 21 (2), 447–462. doi:10.1007/s10098-018-1649-5

Shearer, L., Pap, S., and Gibb, S. W. (2022). Removal of pharmaceuticals from wastewater: a review of adsorptive approaches, modelling and mechanisms for metformin and macrolides. *J. Environ. Chem. Eng.* 10 (4), 108106. doi:10.1016/j.jece.2022.108106

Silva, T. C. F., Vergütz, L., Pacheco, A. A., Melo, L. F., Renato, N. S., and Melo, L. C. A. (2020). Characterization and application of magnetic biochar for the removal of phosphorus from water. *An. Acad. Bras. Ciencias* 92 (3), 201904400–e20190513. doi:10.1590/0001-3765202020190440

Sivaselvam, S., Premasudha, P., Viswanathan, C., and Ponpandian, N. (2020). Enhanced removal of emerging pharmaceutical contaminant ciprofloxacin and pathogen inactivation using morphologically tuned MgO nanostructures. *J. Environ. Chem. Eng.*, 8(5), 104256. doi:10.1016/j.jece.2020.104256

Song, B., Chen, M., Zhao, L., Qiu, H., and Cao, X. (2019). Physicochemical property and colloidal stability of micron- and nano-particle biochar derived from a variety of feedstock sources. *Sci. Total Environ.* 661, 685–695. doi:10.1016/j.scitotenv.2019.01.193

Sun, H., Yang, J., Wang, Y., Liu, Y., Cai, C., and Davarpanah, A. (2021). Study on the removal efficiency and mechanism of tetracycline in water using biochar and magnetic biochar. *Coatings* 11 (11), 1354–1423. doi:10.3390/coatings11111354

Tan, X.-F., Liu, S.-B., Liu, Y.-G., Gu, Y.-L., Wang, X., Liu, S. H., et al. (2017). Biochar as potential sustainable precursors for activated carbon production: multiple applications in environmental protection and energy storage. *Bioresour. Technol.* 227, 359–372. doi:10.1016/j.biortech.2016.12.083

Tomczyk, A., Sokołowska, Z., and Boguta, P. (2020). Biochar physicochemical properties: pyrolysis temperature and feedstock kind effects. *Rev. Environ. Sci. Biotechnol.* 19 (1), 191–215. doi:10.1007/s11157-020-09523-3

Upoma, B. P., Yasmin, S., Ali Shaikh, M. A., Jahan, T., Haque, M. A., Moniruzzaman, M., et al. (2022). A fast adsorption of azithromycin on waste-product-derived graphene oxide induced by H-bonding and electrostatic interactions. *ACS Omega* 7 (34), 29655–29665. doi:10.1021/acsomega.2c01919

Vasudevan, D., Bruland, G. L., Torrance, B. S., Upchurch, V. G., and MacKay, A. A. (2009). pH-dependent ciprofloxacin sorption to soils: interaction mechanisms and soil factors influencing sorption. *Geoderma* 151 (3–4), 68–76. doi:10.1016/j.geoderma.2009.03.007

Wu, M., Feng, Q., Sun, X., Wang, H., Gielen, G., and Wu, W. (2015). Rice (Oryza sativa L) plantation affects the stability of biochar in paddy soil. *Sci. Rep.* 5, 10001–10010. doi:10.1038/srep10001

Xu, Y., Qu, Y., Yang, Y., Qu, B., Shan, R., Yuan, H., et al. (2022). Study on efficient adsorption mechanism of Pb2+ by magnetic coconut biochar. *Int. J. Mol. Sci.* 23 (22), 14053. doi:10.3390/ijms232214053

Yang, X., Zhang, S., Ju, M., and Liu, L. (2019). Preparation and modification of biochar materials and their application in soil remediation. *Appl. Sci. Switz.* 9 (7), 1365. doi:10.3390/app9071365

Yi, Y., Huang, Z., Lu, B., Xian, J., Tsang, E. P., Cheng, W., et al. (2020). Magnetic biochar for environmental remediation: a review. *Bioresour. Technol.* 298, 122468. doi:10.1016/j.biortech.2019.122468

Yu, B., Chang, H., Wei, W., Yu, H., Chen, Z., Cheng, X., et al. (2023). Highly effective removal of ciprofloxacin antibiotic from water by magnetic metal–organic framework. *WaterSwitzerl.* 15 (14), 2531. doi:10.3390/w15142531

Zeng, H., Qi, W., Zhai, L., Wang, F., Zhang, J., and Li, D. (2021). Magnetic biochar synthesized with waterworks sludge and sewage sludge and its potential for methylene blue removal. *J. Environ. Chem. Eng.* 9 (5), 105951. doi:10.1016/j.jece.2021.105951

Zhang, F., Wang, J., Tian, Y., Liu, C., Zhang, S., Cao, L., et al. (2023). Effective removal of tetracycline antibiotics from water by magnetic functionalized biochar derived from rice waste. *Environ. Pollut.* 330 (February), 121681. doi:10.1016/j.envpol.2023.121681

Zhao, C., Ma, J., Li, Z., Xia, H., Liu, H., and Yang, Y. (2020). Highly enhanced adsorption performance of tetracycline antibiotics on KOH-activated biochar derived from reed plants. *RSC Adv.* 10 (9), 5066–5076. doi:10.1039/c9ra09208k

Zhao, X., and Han, R. (2016). Desalination and Water Treatment Characterization of biochar from pyrolysis of wheat straw and its evaluation on methylene blue adsorption. *Environmental Science, Chemistry, Materials Science*. doi:10.1080/19443994.2012.677408

Zhou, Y., Cao, S., Xi, C., Li, X., Zhang, L., Wang, G., et al. (2019). A novel Fe3O4/graphene oxide/citrus peel-derived bio-char based nanocomposite with enhanced adsorption affinity and sensitivity of ciprofloxacin and sparfloxacin. *Bioresour. Technol.*, 292, 121951. doi:10.1016/j.biortech.2019.121951

Zou, C., Wu, Q., Gao, Z., Xu, Z., and Nie, F. (2022). The magnetic porous biochar prepared by K2FeO4-promoted oxidative pyrolysis of bagasse for adsorption of antibiotics in the aqueous solution. *Biomass Convers. Biorefinery*, 0123456789. doi:10.1007/s13399-022-03652-1

Zou, Y., Xu, F., Kong, Q., Shang, D., Zhang, Y., Guo, W., et al. (2020). Pb2+ removal performance by cotton-based and magnetic modified cotton-based biochar prepared from agricultural waste biomass. *Desalination Water Treat.* 207 (January), 246–257. doi:10.5004/dwt.2020.26425